The influence of the Southland Current on circulation patterns within Pegasus Bay

Rafael G. Soutelino[1] and Brett Beamsley[1]
[1] MetOcean Solutions LTD, New Plymouth, New Zealand; r.soutelino@metocean.co.nz

Abstract
The present work evaluates the influence of the Southland Current on the Pegasus Bay (PB) inner and mid shelf circulation using different nesting setups for realistic hydrodynamical hindcasts performed with the Regional Ocean Modelling System (ROMS). The results highlight the importance of the oceanic remote forcing to local flow regime, showing direct and indirect impacts of neglecting such mechanism for PB.

Keywords: Pegasus Bay, Southland Current, coastal sub-inertial currents, modelling.

1. Introduction

The East Coast of New Zealand is a notably complex area in terms of interaction between oceanic and coastal circulation, primarily due to the existence of important western boundary current systems flowing along the continental slopes and outer shelves [1]. Pegasus Bay (PB), located north of Banks Peninsula (BP) has drawn the attention of researchers over the years because of a well-documented interaction between the oceanic flow of the Southland Current (SC) and the shelf and coastal circulation within the bay [2]. Along with being host to an important harbour system and anthropogenic influences, it consists of a scientifically rich oceanographic system. The abrupt changes in geomorphology associated with the BP make it an interesting test-bed for studying the transport of nutrients, larvae and sediment [2].

The SC is a northward/northeast-ward oceanic current that extends from Stewart Island in the south to the Chatham Rise in the north, formed at the subtropical convergence west of New Zealand [3]. On its trajectory along the South Island shelf, most of the SC bends offshore towards the Chatham Rise (Figure 1), but some transport is reported to bend towards PB, in the form of an anticyclonic eddy around BP [4]. [2] were the first to assess the influence of the SC on the nearshore circulation around BP. Those authors analysed ADCP data at sites approximately 2 km offshore South New Brighton to determine whether or not there is quantitative evidence to support the hypothesis of an eddy in PB. Alongshore wind forcing was shown to dominate during energetic wind periods, while during relatively quiescent periods tidal currents and low-frequency residual currents dominate the flow regime. A net southerly alongshore depth-averaged transport is identified; potentially associated with an eddy in PB. In this study, the effect of the SC on circulation in the lee of BP is reassessed with a combination of long term realistic modelling and a new set of in situ measurements. We propose scientific questions such as: (i) what is the contribution of the SC to the total currents on the inner shelf of PB? (ii) what is the impact of poorly introducing the oceanic forcing in modelling efforts to predict the circulation at the inner shelf of PB?, and (iii) what are the implications of underestimating the SC flow in the prediction of arbitrary passive tracers transport and dispersion for a given point source in PB?

2. Methodology

A calibrated 10-year realistic hydrodynamical hindcast targeting optimal representation of the PB circulation was the main strategy to answer the scientific questions enunciated in Section 1. Two different runs were undertaken. A CONTROL run consisted of full spectrum hydrodynamical forcing and a TEST run consisted of a simulation deprived from most of the SC incoming flow in a strategy that will be outlined in the next paragraphs.

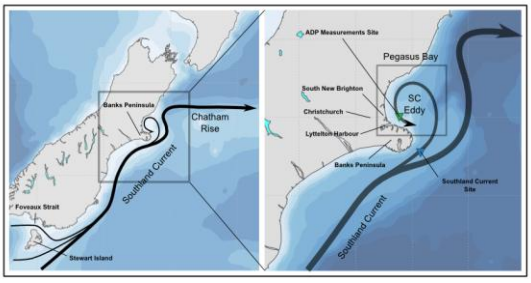

Figure 1: Schematic representation of the main ocean circulation features off the east coast of New Zealand South Island. Main locations and oceanographic features of interest are highlighted. The green triangle is the location of the current meter measurements used in this study. The blue triangle is an arbitrary location within the Southland Current flow domain.

The Regional Ocean Modelling System (ROMS) was used for the hindcast setup [5]. This particular model has been widely used in the scientific and commercial communities to examine hydrodynamic characteristics and phenomena at various spatial scales; from basin, regional and coastal.

Western boundary currents strength and variability are controlled by basin scale and global mechanisms and therefore require careful consideration to ingest correctly into regional and coastal simulations. To accurately represent regional and local scale hydrodynamics it is important that the global dynamics and water mass properties are accounted for and accurately represented at a suitable scale on the higher resolution model boundaries. Additionally, high frequency open boundary feeding is very important to ensure volume conservation and good energy transfer from larger to smaller scales; this has been one of the main reasons for the progress in realistic modelling over the last few years. For example, [4] found that the wind variability in Invercargill (South Island southernmost city) controls the SC variability to a certain order in upstream areas as far as BP, and therefore any realistic modelling effort in the affected areas must properly represent this remote forcing effect.

At a national scale, a ROMS domain encompassing New Zealand at a 0.08° horizontal resolution was nested within the data-assimilative CFSR global reanalysis, with the main goal to accurately capture the basin scale circulation and water mass properties within the NZ context. This domain, hereafter called NZ, is able to more adequately capture the oceanic currents around New Zealand and their variability.

A four-step nesting approach to the hydrodynamical modelling of the PB area was adopted (Figure 2). The CFSR domain (not produced by the present authors) consists of a 35-year global oceanic reanalysis at a 0.5° resolution from the 6-hourly Climate Forecast System Reanalysis (CFSR and CFSv2) products [6], made available by the National Centers for Environmental Prediction (NCEP). An intermediate domain covers the Central East South Island (CESI) with a horizontal resolution of 0.03°. Besides being an essential intermediary step in resolution, the approximate 3 km applied in the CESI domain covers multiple Rossby deformation radii within the deep ocean, allowing for topographic adjustment and more accurate representation of the quasi-geostrophic structure associated with the strength and variability of the SC. This has shown to be crucial to provide the final nest with the right spatial-temporal variability scale of the SC. The final and local grid encompasses the greater PB area (PEGASUS) at a 0.004° horizontal resolution, with the goal to resolve the mid and inner shelves and coastal currents; ultimately providing 3D flow information. The PEGASUS domain extends far enough west and north so that possible grid boundary artefacts are sufficiently distant from the main area of interest, and to properly resolve the coastally trapped waves propagating around BP. Additionally, these extents aim to allow the model to capture the reported flow injections from the SC in the form of topographically-forced anticyclonic eddies and their intrinsic variability.

The 3D flow and mass fields are transferred from the top level domains to the lower level ones by an offline one-way nesting technique [5]. The NZ domain is forced from the CFSR 3D fields at a high frequency 6-hourly interval, and NZ-to-CESI and CESI-to-PEGASUS at a 3-hourly interval. ROMS NZ and CESI domains do not include tides, since they are deeper ocean setups and minimally affected by them.

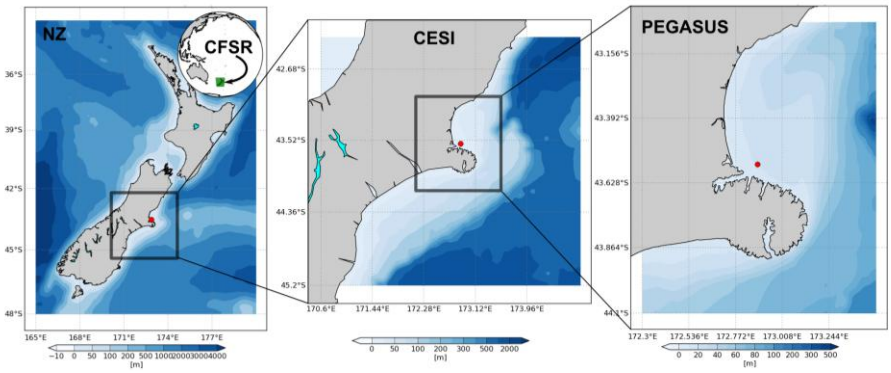

Figure 2: Hydrodynamical hindcast downscaling approach with ROMS. Left panel shows the NZ 0.08° domain, middle panel shows the intermediate 0.03° CESI domain and right panel shows the 0.003° PEGASUS domain. The bathymetry is represented in blue filled contours. The red dot represents the *in situ* observations location.

All domains are submitted to spin-up phases prior to the 10-year hindcast period and/or calibration period, to allow the adjustment of the coarser initial conditions to higher resolution bathymetry and its better resolved topography. The spin-up times are hierarchically established according to the main scales that each one is expected to resolve (Table 1).

The atmospheric forcing for all nests consists of 10-15 km nationwide atmospheric reanalysis produced derived from a WRF model implementation nested within the CFSR atmospheric global reanalysis. Atmospheric variables such as winds, atmospheric pressure, relative humidity, surface temperature, long and short wave radiation and precipitation rate are used at hourly intervals to provide air-sea fluxes to force ROMS in all domains, using a bulk flux parameterization [7].

At the PEGASUS domain scale, tidal forcing (elevations and currents) was introduced using a 5km nation-wide Princeton Ocean Model (POM) 2D tidal solution forced on is boundaries by the Pacific scale Oregon State University Tidal Inverse Solution (OTIS). Tidal currents were not introduced into the coarser scale domains as they are not considered to be the dominant forcing parameter within the deeper shelf environs.

The setup described so far constitutes the CONTROL run. The TEST run skips the NZ and CESI domains, resulting in a highly limited SC contribution to the PEGASUS domain, derived immediately from the 0.5° CFSR 6-hourly fields (Table 2). The CONTROL run was calibrated using a 21-day long (from Feb 21, 2008 to March 12, 2008) *in situ* current meter mooring record located offshore Littleton Harbour (Figure 2). The validation of model against these measurements is shown in Section 3 along with a range of comparisons between CONTROL and TEST simulations skill to predict the measured currents.

Table 1: ROMS nests configuration parameters.

	NZ	CESI	PEGASUS
Resolution	0.08°	0.03°	0.004°
Vertical layers	24	23	18
Open Boundary	CFSR	NZ	CESI
Tidal forcing	No	No	Yes
Atmospheric Forcing	WRF	WRF	WRF
Spin up time	5 years	1 year	3 months

Table 2: Description of the numerical experiments.

CONTROL	CFSR → NZ → CESI → PEGASUS
TEST	CFSR → PEGASUS

3. Results – hydrodynamics

Mean monthly flow patterns for Feb 2008 are used to discuss the importance on characterising the SC flow and how the inclusion of the SC flow affects the circulation in PB.

The main features of the regional oceanography are well represented by ROMS CESI and PEGASUS domains in the CONTROL run (Figure 3).
Within the CESI domain (Figure 3a), the SC dominates the flow south of 44.42°S and clearly bifurcates at 173.39°E, 44.42°S. A coastal branch bends around BP, where some of the water recirculates into PB in the form of an anticyclonic eddy, confirming the observations described in Section 1 [2].

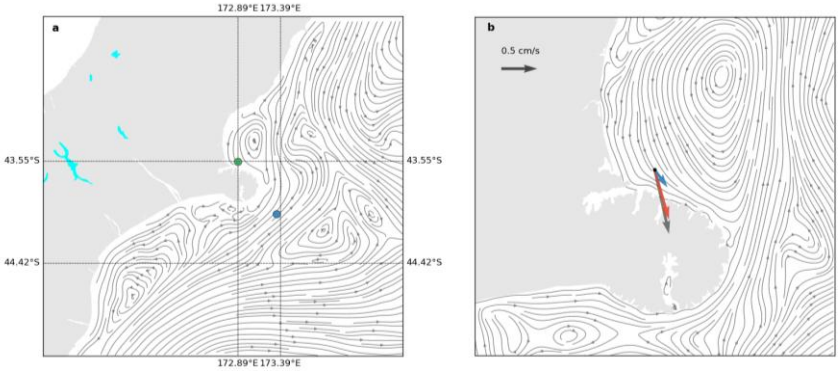

Figure 3: Feb 2008 monthly mean depth-averaged streamfunction for the CESI (a) and PEGASUS (b) ROMS domains. Note the dominance of the Southland Current flow at the offshore area south of Banks Peninsula and the anticyclonic eddy recirculating through Pegasus Bay. The green and blue dots in (a) are respectively the inner shelf Pegasus Bay and offshore Southland current locations which are used to extract modelled alongshore current time series. The green dot coincides with the ADP current measurements site. The arrows in (b) represents the Feb 2008 depth-averaged current vector for the measurements (gray), the CONTROL (red) and TEST (blue) simulations.

The clear effect of the SC in PB circulation can be seen in Figure 3b, showing that the CONTROL setup was able to represent this mechanism. Note the gains in spatial structure from CESI to PEGASUS domains, more notably by the formation of an eastward coastal current south of BP in PEGASUS that is not captured by CESI. This eastward current corroborates well with [9] results, which shows that freshwater plumes south of BP tends to propagate eastwards more often than not.

As can be seen in Figure 3b, there is a substantial difference in the magnitude of the mean currents predicted by the CONTROL and TEST runs (Table 3). The TEST run shows less efficiency in transferring the SC energy from the parent to child nest. Although the mean flow direction towards the SE matches the one in the measurements for the TEST run, the magnitude is substantially smaller. While the average flow of the CONTROL run at the ADP site explained 80% of the observations, the TEST run was only able to explain 33%. Comparing results from CONTROL and TEST experiments, the contribution of the SC to the mean flow in coastal PB is estimated to be around 42%.

Table 3: control/test mean speed comparison.

	Mean current speed	Fraction of the obs
Observations	0.92 cm/s	X
CONTROL	0.72 cm/s	80%
TEST	0.3 cm/s	33%

The depth-averaged current meter records obtained at the ADP location (Figure 3) are exhibited by the black curve in Figure 4. Results are similar to the current climate described by [2], characterising a relatively weak flow regime. Peak tidal currents are of the order of 0.15 m/s with relatively small spring/neap modulation. There is a clear presence of residual flows of the same order of magnitude as the tidal currents, and rarely resulting in total current velocities higher than 0.2 m/s. These residuals are associated with instantaneous, synoptic and mean wind forcing, and also due to the influence of the SC.

The CONTROL simulation (red curves and dots in Figure 4) shows very good skill in reproducing the total current at the ADP location. The residual departures from the tidal flow are notably matched by the model, especially for the events of Feb 23-24 and Mar 2-3. The TEST experiment, however, produced relatively poor results; highlighting the need of accurately capturing the SC in order to define the residual current climate within PB.

Figure 5 shows relevant statistical figures of merit to compare both experiments with respect to the observations. Both setups perform similarly for correlation (probably due to the tidal forcing being identical for both), with the CONTROL run being slightly better. The TEST simulation underestimates the variability quite substantially, while the total variability at the CONTROL run is very similar to the total variability of the measurements. The clearest difference between both simulations is related to the BIAS, which is due to the lack of skill of the TEST setup to reproduce the residual current magnitudes adequately.

The nature of wind forcing is identical in both experiments and therefore the differences between the results for residual currents are not expected to be driven by this component. The only difference between CONTROL and TEST configurations are the way the energy from higher to smaller scales is transferred by the nesting technique, which essentially isolates the contribution of remote forcing from oceanic currents such as the SC.

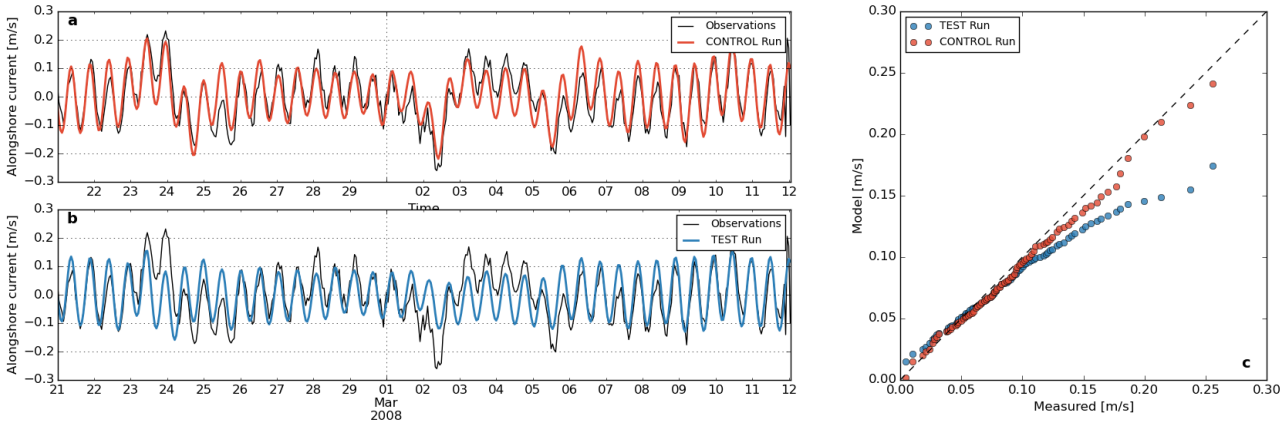

Figure 4: Comparison of the simulation results for CONTROL (red) and TEST (blue) simulations and in situ depth-averaged current measurements. (a) and (b) shows raw time series of the measurements and respective experiment. Note how the CONTROL run (a) has better skill in representing the residual currents that adds up to the tidal flow. The TEST run is clearly underestimating the alongshore current magnitude in stronger residual flow events (c), while the CONTROL simulation shows good overall agreement.

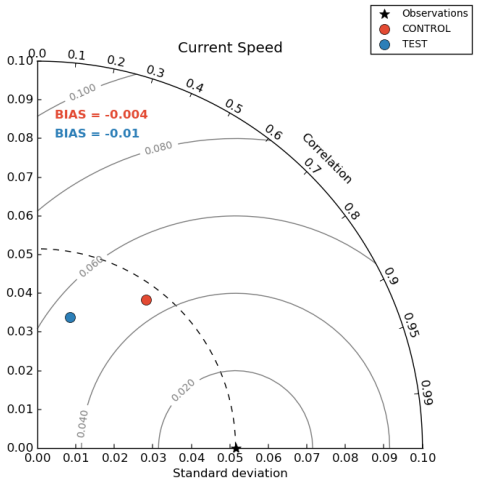

Figure 5: Taylor diagram showing correlation (polar axes) standard deviation (x and y axes) and RMSE (grey contours) between different runs (red and blue dots) and the observations. BIAS are represented in coloured annotations in the upper part of the graph. The closer the dots are to the black star, the better the model skill. Different statistical figures relate to different skills.

To illustrate the response of the local coastal circulation to variability of the SC in the offshore area, alongshore current spectra were computed for two different locations from the CONTROL simulation based in a one-year long time series. The offshore location was chosen based on the average flow shown in Figure 3a (blue circle). The coastal location is the ADP mooring site (green circle). Figure 6 shows the results of this analysis.

The magnitude of the alongshore current is naturally smaller at the coastal location, and there is a clear correlation between the variability events associated with the NE flow SE of BP and SE flow events off PB. It is interesting to note an approximate 20-hour lag between perturbations in the SC and in the PB between the two sites (Figure 6b), which is associated with the time an offshore SC signal takes to propagate around the eddy and reach coastal PB. The spectra (Figure 6c-d) confirms the variability match between both locations, corroborating a clear influence of the SC in the PB circulation. There are significant peaks around typical time scales of western boundary current variability.

4. Results – plumes

A passive tracer point source at the ADP location was introduced in both CONTROL and TEST experiments for a plume scenario in Feb 2008. The tracer concentrations are introduced at the surface at a constant rate of 100 kg m^{-3} h^{-1} during 15 days, and advected and dispersed by the model velocity field without any feedback to the hydrodynamical fields (active tracers - temperature and salinity - and velocity). After 15 days, the tracer release was halted and the model was allowed to evolve for 15 additional days in order to investigate the different dispersion patterns on each setup.

The first 15 days average tracer concentration is given in Figure 7a-b for the CONTROL and TEST

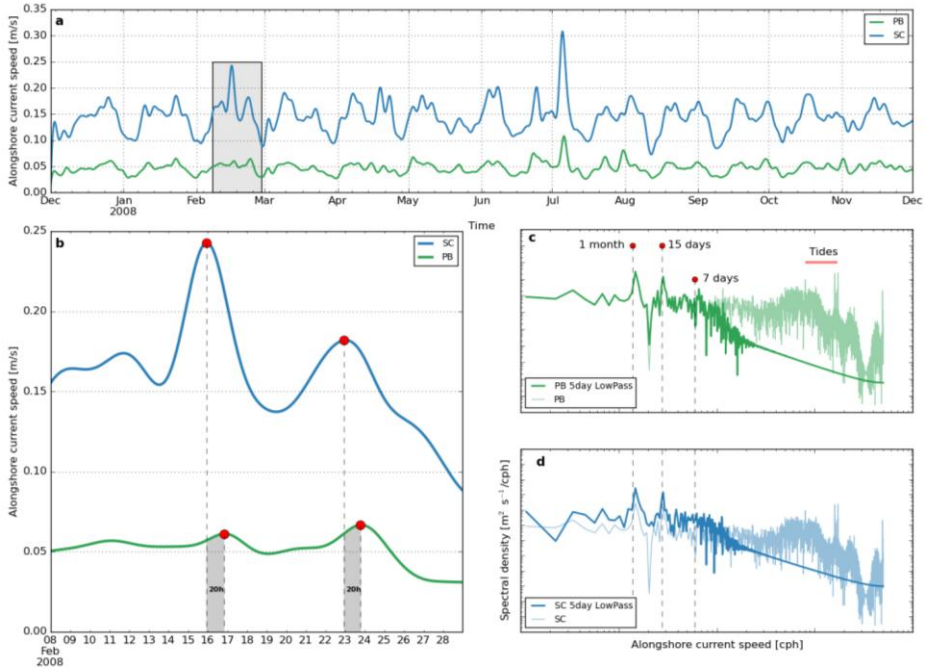

Figure 6: Temporal variability analysis for the alongshore current of CONTROL and TEST simulations at the locations shown in Figure 3. PB stands for Pegasus Bay location and SC for Southland Current location. (a) shows one year alongshore current magnitude filtered with a 5-day low pass Butterworth filter. (b) contains a zoom in two particular alongshore current perturbations. (c) and (d) shows the spectra for each location. Both raw (faded) and 5-day low pass filtered (bold) related spectra are shown.

cases respectively. The passive tracer plume for the CONTROL simulation extends over a greater spatial extent than the TEST run, especially in the SE direction, extending around BP and bending towards the W. It is also noted that the CONTROL run forced dispersion of the tracer to the north more effectively than the TEST run.

The TEST run tends to overestimate the tracer concentration with respect to CONTROL in the near field due to the lack of stronger residual currents to mix and advect the plume, and hence underestimates the concentrations in the far field.

The concentrations 15 days after the tracer release interruption are given in Figure 7 d-f for the CONTROL, TEST and difference respectively. Overall, in both setups, the concentrations decreased from about 5 log (kg/m^{-3}) in the near field to less than 2 log (kg/m^{-3}). Note that the CONTROL model comparatively produces a more alongshore-elongated plume, reaching areas W of BP.

Neglecting and/or poorly representing the SC influence to the coastal PB can clearly influence the propagation of passive tracers in a short time scale. These results suggest that the failure to represent the SC may result in misleadingly more confined contaminant plumes in a release in the lee of BP.

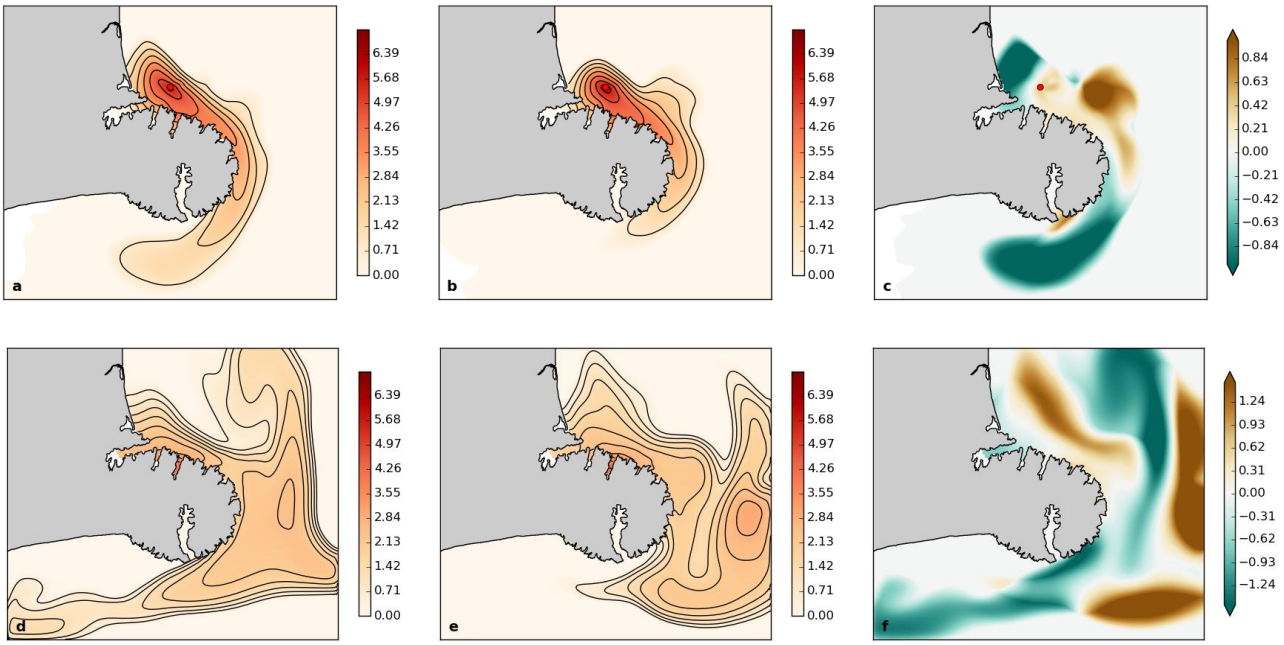

Figure 7: Results of passive tracer plume dispersion for both CONTROL and TEST experiments. (a,b) shows the log of average tracer concentration during the first 15 days of release. The red dot in the upper panels shows the release source. (d,e) shows the passive tracer log concentration in the last day of simulation – 15 after the release interruption. (c) and (f) shows the difference between TEST and CONTROL concentrations shown in (a,b) and (d,e), respectively.

5. Summary

A realistic ocean hindcast deprived of the SC flow was used in comparison with a fully forced and validated simulation to quantify the SC role.

The absence of the SC forcing greatly affects the total currents in the inner shelf of PB, with magnitudes of the residual currents reduced by nearly half when compared to the fully forced model. The known net south-eastward transport in PB is not achieved successfully with the absence of the SC.

The quantitative influence of the SC based on the long term model data was established by similar spectrum characteristics of alongshore currents NE off Littleton Harbour and SE of Banks Peninsula (BP). Perturbations in the PB occur 20 h after perturbations in the SC off SE BP, with decay in magnitude of approximately a factor of 4. Moreover, the careful downscaling approach used in the nesting technique has shown to be fundamental to transfer larger scale energy of the SC to the inner shelf of PB. When intermediate nests were skipped, this downscale cascade was unsatisfactory.

6. Acknowledgements

We thank the Lyttelton Port of Christchurch for making the measurements available and the ROMS scientific community.

7. References

[1] Rickard, G.J., Hadfield M.G. and Roberts M.J. (2005). Development of a regional ocean model for New Zealand. New Zealand Journal of Marine and Freshwater Research, 39(5) 1171-1191.

[2] Reynolds-Fleming, J. V. and Fleming, J. G. (2005). Coastal circulation within the Banks Peninsula region, New Zealand. New Zealand Journal of Marine and Freshwater Research, 39, 217-225.

[3] Chiswell, M. (1996). Variability in the Southland Current, New Zealand. New Zealand Journal of Marine and Freshwater Research, 30, 1-17.

[4] Carter, L. and Herzer. R, H. (1979). The hydraulic regime and its potential to transport sediment on the Canterbury continental shelf. New Zealand Oceanographic Memoir 83, 33.

[5] Haidvogel, D. B. et al (2008). Ocean forecasting in terrain-following coordinates: Formulation and skill assessment of the Regional Ocean Modeling System. Journal of Computational Physics 227(7), 3595-3624.

[6] Saha, E. et al (2010). The NCEP Climate Forecast System Reanalysis. Bull. Am. Meteorol. Soc. 91, 1015–1057.

[7] Fairall, C. W., E. F. Bradley, J. E. Hare, A. A. Grachev and J. B. Edson (2003): Bulk parameterization of air-sea fluxes: Updates and verification for the COARE algorithm. J. Clim., 16 (4) 571-591.

[8] Egbert, G. D and Erofeeva, S. Y. (2002). Efficient inverse modeling of barotropic ocean tides. Journal of Atmospheric and Ocean Technology. 19 183-204.

[9] Hadfield, M. and Zeldis, J. (2012). Freshwater dilution and transport in Canterbury Bight. Technical Report. NIWA. 39 pp.